



UNIVERSITY OF LEEDS

This is a repository copy of *Energy Detection Based Spectrum Sensing Over k - μ and k - μ Extreme Fading Channels*.

White Rose Research Online URL for this paper:
<http://eprints.whiterose.ac.uk/109522/>

Version: Accepted Version

Article:

Sofotasios, PC, Rebeiz, E, Zhang, L et al. (3 more authors) (2013) Energy Detection Based Spectrum Sensing Over k - μ and k - μ Extreme Fading Channels. *IEEE Transactions on Vehicular Technology*, 62 (3). pp. 1031-1040. ISSN 0018-9545

<https://doi.org/10.1109/TVT.2012.2228680>

© 2012 IEEE. Personal use of this material is permitted. Permission from IEEE must be obtained for all other uses, in any current or future media, including reprinting/republishing this material for advertising or promotional purposes, creating new collective works, for resale or redistribution to servers or lists, or reuse of any copyrighted component of this work in other works.

Reuse

Items deposited in White Rose Research Online are protected by copyright, with all rights reserved unless indicated otherwise. They may be downloaded and/or printed for private study, or other acts as permitted by national copyright laws. The publisher or other rights holders may allow further reproduction and re-use of the full text version. This is indicated by the licence information on the White Rose Research Online record for the item.

Takedown

If you consider content in White Rose Research Online to be in breach of UK law, please notify us by emailing eprints@whiterose.ac.uk including the URL of the record and the reason for the withdrawal request.



eprints@whiterose.ac.uk
<https://eprints.whiterose.ac.uk/>

Energy Detection–Based Spectrum Sensing over $\kappa-\mu$ and $\kappa-\mu$ *Extreme* Fading Channels

P. C. Sofotasios, *Member, IEEE*, E. Rebeiz, *Student Member, IEEE*,
L. Zhang, *Member, IEEE*, T. A. Tsiftsis, *Senior Member, IEEE*,
S. Freear, *Senior Member, IEEE*, and D. Cabric, *Member, IEEE*

Abstract

Energy detection is a simple and popular method of spectrum sensing in cognitive radio systems. It is widely known that the performance of sensing techniques is largely affected when users experience fading effects. This paper investigates the performance of an energy detector over the generalized $\kappa-\mu$ and $\kappa-\mu$ *Extreme* fading channels which have been shown to provide remarkably accurate fading characterization. Novel analytic expressions are derived for the corresponding average probability of detection for the case of single user detection. These results are subsequently extended to the case of square-law selection (SLS) diversity as well as for collaborative detection. As expected the performance of the detector is highly dependant upon the severity of fading since even small variation of the fading conditions affect significantly the corresponding average probability of detection. Furthermore, the performance of the detector improves substantially as the number of branches, or collaborating users, increase in both severe and moderate fading conditions while it is shown that the $\kappa-\mu$ *Extreme* model is capable of accounting for fading variations even at low signal-to-noise (SNR) values. The offered results are particularly useful in assessing the effect of fading in energy detection-based cognitive radio communication systems and thus can be used to quantify the tradeoffs between the sensing performance and energy efficiency of cognitive radio networks.

This work was supported in part by the Engineering and Physical Sciences Research Council (EPSRC).

P. C. Sofotasios, L. X. Zhang and S. Freear are with the School of Electronic and Electrical Engineering, University of Leeds, LS2 9JT Leeds, UK (e-mail: {p.sofotasios; l.x.zhang; s.freear}@leeds.ac.uk)

T. A. Tsiftsis is with the Department of Electrical Engineering, Technological Educational Institute of Lamia, 35100 Lamia, Greece (e-mail: tsiftsis@teilam.gr)

E. Rebeiz and D. Cabric are with the Department of Electrical Engineering, University of California at Los Angeles, 56-125B Engineering IV, Los Angeles, CA 90095-1594, USA. (e-mail: {rebeiz; danijela}@ee.ucla.edu).

Index Terms

Spectrum sensing, energy detector, fading channels, unknown signal detection, collaborative spectrum sensing, κ - μ fading, diversity.

I. INTRODUCTION

The detection of unknown signals is an important topic of wireless communications. It is typically realized in the form of spectrum sensing with energy detection (ED) constituting the most simple and popular approach. The operating principle of ED is based on the deployment of a radiometer which is a non-coherent detection device that measures the energy level of a received signal waveform over an observation time window. Then, it compares it with a pre-defined energy threshold and determines whether an unknown signal is present or absent [1]–[3].

H. Urkowitz was the first to address the problem of detecting unknown signals over a flat band-limited Gaussian noise channel as he comprehensively derived analytic expressions for the probability of detection and the probability of false alarm metrics [4]. These metrics are based on the assumption that the decision statistics follow the central chi-square and the non-central chi-square distribution, respectively. A few decades later, this problem was revisited by Kostylev who considered quasi-deterministic signals operating in fading environments [5]. Thanks to its low implementation complexity and no requirements for knowledge of the signal, the ED method has been widely associated with applications in RADAR systems while it has been also shown to be largely applicable in emerging wireless technologies such as ultra-wideband communications and cognitive radio [6], [7]. In the former, the energy detector is exploited for borrowing an idle channel from authorized users, whereas in the latter it identifies the presence or absence of a deterministic signal and decides whether a primary user is active or idle. According to the corresponding decision, the secondary user either remains silent, or proceeds in utilizing the unoccupied band until the state of the primary user becomes active [1], [8]. This opportunistic method has been extensively shown to substantially increase the utilization of the already allocated radio spectrum, offering a considerable mitigation of the currently extensive spectrum scarcity [9].

Capitalizing on the above, numerous studies have been devoted to the analysis of the performance of energy detection-based spectrum sensing in different communication scenarios. Specifically, the authors in [10] derived closed-form expressions for the average probability

of detection in Rayleigh, Rice and Nakagami fading channels for both single-channel and multi-channel scenarios. Likewise, the ED performance in the case of equal gain combining and Nakagami- m multipath fading has been investigated in [11] whereas the corresponding performance in collaborative spectrum sensing and in relay-based cognitive radio networks has been assessed in [12]–[16]. A novel semi-analytic method for evaluating the performance of energy detection of unknown deterministic signals was reported in [17]. This important work is based on the moment-generating-function (MGF) method and aims to overcome the analytical difficulties that arise from the presence of the Marcum Q-function. This method was utilized in the case of maximum-ratio combining (MRC) in the presence of Rayleigh, Rice and Nakagami- m fading in [17] as well as for the useful case of correlated Rayleigh and Rician fading channels in [18]. Finally, the detection of unknown signals in low SNR and in K -distributed (K), generalized K (K_G) and the very flexible η - μ fading channels has been recently analyzed in [19]–[22].

The κ - μ distribution is a generalized fading model that is distinctive for providing adequate characterisation of multipath fading particularly for line-of-sight (LOS) communication scenarios. It was reported in [23] along with the η - μ fading model which accounts for non-line-of-sight (NLOS) communication conditions. The κ - μ fading model has been shown to be particularly flexible and it includes as special cases the well known Rice, Nakagami- m , Rayleigh and one-sided Gaussian distributions [23]. Its remarkable flexibility and usefulness are shown clearly in [23, Fig. 9]. The known η - μ fading model is also depicted and one can notice how the two models complement each-other. It also evident from this Figure that the κ - μ fading model significantly outperforms the characterization capabilities of Rice, Nakagami- m and Rayleigh distributions. Furthermore, it constitutes the basis for deriving the κ - μ *Extreme* distribution which is a recently proposed remarkable fading model that provides accurate characterization of radio propagation under severe fading conditions. Importantly, it has been shown that these conditions, even worse than Rayleigh, typically occur in enclosed environments such as airplanes, trains, buses and shopping malls [24], [25].

Nevertheless, in spite of the undoubted usefulness of the κ - μ and κ - μ *Extreme* fading models, no studies related to the detection of unknown signals in these fading channels have been reported in the open research literature. Motivated by this, this work is devoted to the analysis of energy detection over κ - μ and κ - μ *Extreme* fading channels. Specifically, novel analytic expressions are firstly derived for the average probability of detection for the conventional single

user scenario. Subsequently, these expressions are extended to account for the collaborative energy detection as well as for the square-law-selection (SLS) diversity scheme. As expected, the performance of the energy detector is highly dependant upon the value of the κ and μ parameters. This is evident in the whole average signal-to-noise (SNR) range, and particularly the positive regime, as even small variations of the fading conditions affect significantly the performance of the corresponding average probability of detection. In addition, it is shown that the κ - μ *Extreme* model appears capable of accounting for fading variations even at low signal-to-noise (SNR) values. Finally, it shown, that the detector's performance is, as expected, substantially improved in both severe and moderate fading conditions as the number of diversity paths or number of users increase. Therefore, the offered results enable us to quantify the effect of fading in the system performance in various communication scenarios and thus to determine the required power levels for ensuring robust and accurate performance of energy detectors combined with sufficient benefits in terms of energy efficiency.

The remainder of this paper is organized as follows: The system and channel model are described in Section II. The average detection probabilities of the energy detector over κ - μ and κ - μ *Extreme* channels are analyzed in Sections III and IV, respectively. Numerical results for each communication scenario along with necessary discussions are provided in Section V, while closing remarks are given in Section VI.

II. SYSTEM MODEL AND CHANNEL MODEL

A. Energy Detection

In narrowband energy detection, the received signal waveform follows a binary hypothesis that can be represented as [18, eq. (1)],

$$r(t) = \begin{cases} n(t) & : H_0 \\ hs(t) + n(t) & : H_1 \end{cases} \quad (1)$$

where $s(t)$ is an unknown deterministic signal whereas h is the amplitude of the channel coefficient and $n(t)$ is a white Gaussian noise process. The samples of $n(t)$ are assumed to be zero-mean Gaussian random variables with variance N_0W with W and N_0 denoting the single-sided signal bandwidth and a single-sided noise power spectral density, respectively [18].

The hypotheses H_0 and H_1 refer to the cases that a signal is absent or present, respectively. The received signal is subject to filtering, squaring and integration over the time interval T which is expressed as [10, eq. (2)], $y \triangleq \frac{2}{N_0} \int_0^T |r(t)|^2 dt$.

The output of the integrator is a measure of the energy of the received waveform which acts as a test statistic that determines whether the received energy measure corresponds only to the energy of noise (H_0) or to the energy of both the unknown deterministic signal and noise (H_1). By denoting the time bandwidth product as $u = TW$, the test statistic follows the central chi-square distribution with $2u$ degrees of freedom under the H_0 hypothesis and the non central chi-square distribution with $2u$ degrees of freedom under the H_1 hypothesis [4]. To this effect, the corresponding probability density function (pdf) in the presence of *Additive-white-Gaussian-noise* (AWGN) is given by [10, eq. (3)],

$$p_Y(y) = \begin{cases} \frac{1}{2^u \Gamma(u)} y^{u-1} e^{-\frac{y}{2}} & : H_0 \\ \frac{1}{2} \left(\frac{y}{2\gamma} \right)^{\frac{u-1}{2}} e^{-\frac{y+2\gamma}{2}} I_{u-1}(\sqrt{2y\gamma}) & : H_1 \end{cases} \quad (2)$$

where $\gamma \triangleq h^2 E_s / N_0$ denotes the SNR, $u = TW$ is the time bandwidth product and E_s, T are the signal energy and the observation time interval, respectively. Also, $\Gamma(a) \triangleq \int_0^\infty t^{a-1} e^{-t} dt$ is the Euler's gamma function while $I_n(x) \triangleq \frac{1}{\pi} \int_0^\pi \cos(n\theta) e^{x \cos(\theta)} d\theta$ is the modified Bessel function of the first kind [26].

As already mentioned, an energy detector is largely characterised by a predefined energy threshold, λ . This threshold is critical in the decision process and is promptly associated to three measures that overall evaluate the performance of the detector: i) the probability of false alarm, $P_f = Pr(y > \lambda | H_0)$; ii) the probability of detection, $P_d = Pr(y > \lambda | H_1)$ and iii) the missed detection probability, $P_m = 1 - P_d$. The first two measures are deduced by integrating (2) over zero to infinity yielding [10]

$$P_f = \frac{\Gamma\left(u, \frac{\lambda}{2}\right)}{\Gamma(u)} \quad (3)$$

and

$$P_d = Q_u(\sqrt{2\gamma}, \sqrt{\lambda}) \quad (4)$$

where $\Gamma(a, x) \triangleq \int_x^\infty t^{a-1} e^{-t} dt$ and $Q_m(a, b) \triangleq \frac{1}{a^{m-1}} \int_b^\infty x^m e^{-\frac{x^2+a^2}{2}} I_{m-1}(ax) dx$ denote the upper incomplete gamma function and the generalized Marcum Q-function, respectively [26], [27].

B. The κ - μ Fading Model

As already mentioned in Sec. I, the κ - μ fading model has been shown to represent effectively the small-scale variations of a fading signal in NLOS communications. Physically, the κ - μ fading model considers a signal composed of clusters of multipath waves, propagating in a non-homogeneous environment. Within any one cluster, the phases of the scattered waves are random and have similar delay times with delay-time spreads of different clusters being relatively large. The clusters of multipath waves are assumed to have scattered waves with identical powers while each cluster consists of a dominant component with arbitrary power. To this effect, the parameters μ and κ correspond to the number of multipath clusters and the ratio between the total power of the dominant components and the total power of the scattered waves, respectively. These two parameters render this model remarkably flexible as its capturing range is particularly broad [23, Fig. 9]. This is also evident by the fact that the widely known Rice and Nakagami- m fading models are included as special cases for $\mu = 1$ and $\kappa = 0$, respectively [23]. Therefore, this model can provide a meaningful insight on how fading affects the performance of an energy detector which ultimately leads to a significant improvement on the design of cognitive radio system in terms of energy efficiency and cost.

For a fading signal with envelope $P = R/\hat{r}$ and $\hat{r} = \sqrt{E(R^2)}$, the envelope pdf of κ - μ distribution is expressed as [23, eq. (1)],

$$p_P(r) = \frac{2\mu(\kappa+1)^{\frac{\mu+1}{2}}}{\kappa^{\frac{\mu-1}{2}} e^{\mu\kappa}} \frac{r^\mu}{\hat{r}^{\mu+1}} e^{-\mu(1+\kappa)\frac{r^2}{\hat{r}^2}} I_{\mu-1} \left(2\mu\sqrt{\kappa(\kappa+1)}\frac{r}{\hat{r}} \right) \quad (5)$$

where $E(R)$ denotes expectation and \hat{r} is the root-mean-square (rms) value of R . The corresponding pdf of instantaneous SNR per symbol γ is given by [23, eq. (10)],

$$p_\gamma(\gamma) = \frac{\mu(\kappa+1)^{\frac{\mu+1}{2}} e^{-\mu\kappa}}{\bar{\gamma}\kappa^{\frac{\mu-1}{2}} e^{\mu(1+\kappa)\frac{2}{\bar{\gamma}}}} \left(\frac{\gamma}{\bar{\gamma}} \right)^{\frac{\mu-1}{2}} I_{\mu-1} \left(2\mu\sqrt{\kappa(\kappa+1)}\frac{\gamma}{\bar{\gamma}} \right) \quad (6)$$

where $\bar{\gamma}$ represents the average SNR per symbol. Finally, the parameters κ and μ are related to each-other by the following relationship [23],

$$\mu = \frac{E^2(R^2)}{\text{Var}(R^2)} \frac{1 + 2\kappa}{(1 + \kappa)^2} = \frac{E^2(P)}{\text{Var}(P)} \frac{1 + 2\kappa}{(1 + \kappa)^2} \quad (7)$$

with $\text{Var}(\cdot)$ denoting mathematical variance.

III. AVERAGE DETECTION PROBABILITY OVER κ - μ FADING CHANNELS

It is recalled that (3) and (4) account for the case of AWGN channels. For communication scenarios over fading channels the average probability of detection is obtained by averaging (4) over the corresponding SNR fading statistics, namely,

$$\overline{P}_d = \int_0^\infty Q_u(\sqrt{2\gamma}, \sqrt{\lambda}) p_\gamma(\gamma) d\gamma. \quad (8)$$

Based on this, analytic expressions for the case of Rayleigh, Rice, Nakagami- m , K , K_G , log-normal and η - μ fading channels where derived in [8]–[14], [17]–[22]. Therefore, the average probability of detection in the case of generalized κ - μ fading can be obtained by averaging (4) over the statistics of (6). To this effect, by substituting (6) in (8) yields,

$$\overline{P}_{d\kappa-\mu} = \frac{\mu(\kappa+1)^{\frac{\mu+1}{2}}}{\kappa^{\frac{\mu-1}{2}} e^{\mu\kappa} \bar{\gamma}^{\frac{\mu+1}{2}}} \int_0^\infty \gamma^{\frac{\mu-1}{2}} Q_u(\sqrt{2\gamma}, \sqrt{\lambda}) e^{-\mu(1+\kappa)\frac{\gamma}{\bar{\gamma}}} I_{\mu-1}\left(2\mu\sqrt{\kappa(\kappa+1)\frac{\gamma}{\bar{\gamma}}}\right) d\gamma. \quad (9)$$

An analytic expression for (9) can be derived by expressing the involved Marcum Q-function according to [28, eq. (29)] and [29, eq. (6)], as follows¹

$$Q_u(\sqrt{2\gamma}, \sqrt{\lambda}) = e^{-\gamma} \sum_{l=0}^{\infty} \frac{\gamma^l \Gamma(l+u, \frac{\lambda}{2})}{\Gamma(l+1)\Gamma(l+u)}. \quad (10)$$

Hence, by substituting (10) into (9) $\overline{P}_{d\kappa-\mu}$ can be re-written as,

$$\overline{P}_{d\kappa-\mu} = \frac{\mu(\kappa+1)^{\frac{\mu+1}{2}}}{\kappa^{\frac{\mu-1}{2}} e^{\mu\kappa} \bar{\gamma}^{\frac{\mu+1}{2}}} \sum_{l=0}^{\infty} \frac{\Gamma(l+u, \frac{\lambda}{2})}{\Gamma(l+1)\Gamma(l+u)} \underbrace{\int_0^\infty \gamma^{\frac{\mu-1}{2}+l} e^{-\gamma(1+\frac{\mu(1+\kappa)}{\bar{\gamma}})} I_{\mu-1}\left(2\mu\sqrt{\kappa(\kappa+1)\frac{\gamma}{\bar{\gamma}}}\right) d\gamma}_{\mathcal{I}_1}. \quad (11)$$

¹One can alternatively use the accurate polynomial approximation in [29, eq. (7)], [41, eq. (3.39)] which reduces to [29, eq. (7)] for $k \rightarrow \infty$.

Notably, the above integral is identical to [30, eq. (6.643.2)] which can be expressed in terms of the Whittaker hypergeometric function, $M_{\nu,\mu}(z)$ given by,

$$\mathcal{I}_1 = (\mu)_l e^{\frac{\kappa(1+\kappa)\mu^2}{\bar{\gamma}+\mu(1+\kappa)}} M_{-\frac{1}{2}-l, \frac{\mu}{2}-\frac{1}{2}} \left(\frac{\kappa(1+\kappa)\mu^2}{\bar{\gamma}+\mu(1+\kappa)} \right) \quad (12)$$

where $(\mu)_l \triangleq \Gamma(\mu+l)/\Gamma(\mu)$ is the Pochhammer symbol [26]. With the aid of [30, eq. (9.220.2)], equation (12) can be equivalently expressed as

$$\mathcal{I}_1 = (\mu)_l \mu^\mu \kappa^{\frac{\mu}{2}} (1+\kappa)^{\frac{\mu}{2}} {}_1F_1 \left(\mu+l; \mu; \frac{\kappa(1+\kappa)\mu^2}{\bar{\gamma}+\mu(1+\kappa)} \right). \quad (13)$$

where ${}_1F_1(a; b; x)$ is the Kummer's confluent hypergeometric function [26]. Hence, by substituting (13) into (11), the following infinite series representation for $\overline{P}_{d\kappa-\mu}$ is deduced:

$$\overline{P}_{d\kappa-\mu} = \sum_{l=0}^{\infty} \frac{\mu^\mu (1+\kappa)^\mu e^{-\mu\kappa} \Gamma(l+\mu) \bar{\gamma}^l \Gamma(l+u, \frac{\lambda}{2})}{\Gamma(l+1) \Gamma(u+l) \Gamma(\mu) (\bar{\gamma}+\mu+\kappa\mu)^{\mu+l}} {}_1F_1 \left(\mu+l; \mu; \frac{\kappa(1+\kappa)\mu^2}{\bar{\gamma}+\mu(1+\kappa)} \right). \quad (14)$$

Importantly, the above expression can be expressed in closed-form as follows:

$$\overline{P}_{d\kappa-\mu} = \frac{\mu^\mu (1+\kappa)^\mu e^{-\mu\kappa}}{(\bar{\gamma}+\mu+\kappa\mu)^\mu} \left\{ F_A \left(\mu; 1; \mu, 1; \frac{\bar{\gamma}}{\bar{\gamma}\mu+\kappa\mu}, \frac{\kappa(1+\kappa)\mu^2}{\bar{\gamma}+\mu(1+\kappa)} \right) - \frac{\lambda^u}{u! 2^u} H_A \left(\mu, u; u, u+1, \mu; \frac{\lambda\bar{\gamma}}{2(\bar{\gamma}+\mu+\kappa\mu)}; -\frac{\lambda}{2}; \frac{\kappa(1+\kappa)\mu^2}{\bar{\gamma}+\mu(1+\kappa)} \right) \right\}. \quad (15)$$

where $F_A()$ and $H_A()$ denote the Lauricella hypergeometric function of two variables and the complete triple hypergeometric function of the first kind, respectively [30], [33]–[36]. A detailed proof of (15) is provided in APPENDIX A.

A. Square-Law Selection (SLS)

Square-Law selection, also known as selection combining, is an efficient diversity scheme that is highly regarded for its simple realization. Its principle of operation is based on selecting the output of the branch with maximum decision statistic, $y_{SLS} = \max\{y_1, y_2, \dots, y_L\}$, [31]. Based on this, the corresponding \overline{P}_d in the case of $\kappa-\mu$ fading can be obtained by averaging P_d^{SLS} in [10, eq. (15)] over L independent $\kappa-\mu$ branches, namely,

$$\overline{P}_{d_{\kappa-\mu}}^{SLS} = 1 - \prod_{i=1}^L \int_0^{\infty} \left[1 - Q_u \left(\sqrt{2\gamma_i}, \sqrt{\lambda} \right) \right] p_{\gamma_i}(\gamma_i) d\gamma_i. \quad (16)$$

Therefore, by substituting (6) in (16) it follows that

$$\overline{P}_{d_{\kappa-\mu}}^{SLS} = 1 - \prod_{i=1}^L \left[\int_0^{\infty} p_{\gamma_i}(\gamma_i) d\gamma_i - \int_0^{\infty} Q_u \left(\sqrt{2\gamma_i}, \sqrt{\lambda} \right) p_{\gamma_i}(\gamma_i) d\gamma_i \right]. \quad (17)$$

By recalling that $\int_0^{\infty} p(\gamma) d\gamma \triangleq 1$, it is noticed that the integral that needs to be evaluated in (17) is the same as the integral in (9). Therefore, by following the same procedure as in the derivation of $\overline{P}_{d_{\kappa-\mu}}$, a closed-form expression for (17) is deduced,

$$\begin{aligned} \overline{P}_{d_{\kappa-\mu}}^{SLS} &= 1 - \prod_{i=1}^L \left\{ 1 - \overline{P}_{d_{\kappa-\mu}}(\gamma_i) \right\} \\ &= 1 - \prod_{i=1}^L \left\{ 1 - \frac{\mu^\mu (1 + \kappa)^\mu e^{-\mu\kappa}}{(\overline{\gamma}_i + \mu + \kappa\mu)^\mu} \left[F_A \left(\mu; 1; \mu, 1; \frac{\overline{\gamma}_i}{\overline{\gamma}_i\mu + \kappa\mu}, \frac{\kappa(1 + \kappa)\mu^2}{\overline{\gamma}_i + \mu(1 + \kappa)} \right) \right. \right. \\ &\quad \left. \left. - \frac{\lambda^u}{u!2^u} H_A \left(\mu, u; u, u + 1, \mu; \frac{\lambda\overline{\gamma}_i}{2(\overline{\gamma}_i + \mu + \kappa\mu)}; -\frac{\lambda}{2}; \frac{\kappa(1 + \kappa)\mu^2}{\overline{\gamma}_i + \mu(1 + \kappa)} \right) \right] \right\}. \end{aligned} \quad (18)$$

As always, the corresponding P_f is independent of the fading statistics and is given by [10, eq. (14)], namely,

$$P_f^{SLS} = 1 - \left[1 - \frac{\Gamma(u, \frac{\lambda}{2})}{\Gamma(u)} \right]^L. \quad (19)$$

B. Collaborative Detection

It has been extensively shown in the research literature that the performance of energy detection based spectrum sensing can be significantly improved when secondary users collaborate by sharing their information. In this case, the probability of detection and probability of false-alarm for a scenario with n collaborating users are given by $Q_d \triangleq 1 - (1 - P_d)^n$ and $Q_f \triangleq 1 - (1 - P_f)^n$, respectively [13]. Based on this, the average probability of detection of a system with no diversity and $\kappa-\mu$ fading in a collaborative scenario n -users is given by

$$\begin{aligned}
\overline{Q}_{d_{\kappa-\mu}} &= 1 - [1 - \overline{P}_{d_{\kappa-\mu}}]^n \\
&= 1 - \left[1 - \frac{\mu^\mu (1 + \kappa)^\mu e^{-\mu\kappa}}{(\overline{\gamma} + \mu + \kappa\mu)^\mu} \left\{ F_A \left(\mu; 1; \mu, 1; \frac{\overline{\gamma}}{\overline{\gamma}\mu + \kappa\mu}, \frac{\kappa(1 + \kappa)\mu^2}{\overline{\gamma} + \mu(1 + \kappa)} \right) \right. \right. \\
&\quad \left. \left. - \frac{\lambda^u}{u!2^u} H_A \left(\mu, u; u, u + 1, \mu; \frac{\lambda\overline{\gamma}}{2(\overline{\gamma} + \mu + \kappa\mu)}; -\frac{\lambda}{2}; \frac{\kappa(1 + \kappa)\mu^2}{\overline{\gamma} + \mu(1 + \kappa)} \right) \right\} \right]^n.
\end{aligned} \tag{20}$$

IV. ENERGY DETECTION OVER κ - μ EXTREME FADING CHANNELS

A. The κ - μ Extreme Fading Model

As already mentioned in Sec. I, the κ - μ *Extreme* distribution was recently proposed as a fading model that is capable of accounting adequately for severe fading conditions which are mainly encountered in enclosed environments such as airplanes, buses, trains and shopping malls, [24], [25]. Unlike propagation in traditional outdoor and indoor environments, propagation in enclosed environments has been shown to present only a small number of multipath components. To this effect, the use of the Central Limit Theorem (CLT) becomes inappropriate and as a consequence, the corresponding wireless channel can not be accurately characterized by the well known small-scale fading distributions such as Rayleigh, Nakagami- m , Hoyt and Weibull [24], [25], [32].

The κ - μ *Extreme* distribution emerges as a special case of the κ - μ distribution and its normalized pdf is given by [25, eq. (6)], namely,

$$p_\rho(\rho) = 4me^{-2m(1+\rho^2)} I_1(4m\rho) + e^{-2m}\delta(\rho) \tag{21}$$

where $m = \text{Var}^{-1}(R^2)$ is the Nakagami- m parameter and $\delta(\rho)$ denotes for the Dirac delta function [26]. According to [25, eq. (13)] and with the aid of [23, eq. (10)], the corresponding power pdf is expressed as follows:

$$p_\gamma(\gamma) = \frac{2m}{\sqrt{\gamma\overline{\gamma}}} e^{-2m(1+\frac{\gamma}{\overline{\gamma}})} I_1 \left(4m\sqrt{\frac{\gamma}{\overline{\gamma}}} \right) + \frac{e^{-2m}}{2\sqrt{\gamma\overline{\gamma}}} \delta(\gamma). \tag{22}$$

B. Average Detection Probability in κ - μ Extreme Fading

The average detection probability in the presence of κ - μ *Extreme* fading, $\overline{P}_{d_{\kappa-\mu Ext.}}$, can be derived by following the same procedure as in the derivation of $\overline{P}_{d_{\kappa-\mu}}$ in Sec. III. To this end,

by substituting (22) into (8), setting $x = \sqrt{2\gamma}$ and noticing that due to the $\delta(\rho)$ function the second term in (22) reduces to zero for $\gamma \neq 0$, one obtains

$$\overline{P}_{d\kappa-\mu Ext.} = \frac{2\sqrt{2m}}{\sqrt{\gamma}e^{2m}} \underbrace{\int_0^\infty Q_u(x, \sqrt{\lambda}) e^{-\frac{m}{\gamma}x^2} I_1 \left(2m\sqrt{\frac{2}{\gamma}}x \right) dx}_{\mathcal{I}_2}. \quad (23)$$

Notably, the above integral belongs to the same class as the \mathcal{I}_1 integral. To this effect, by setting $x = \sqrt{2\gamma}$ in (10) and substituting in (23) yields the following analytic expressions for \mathcal{I}_2 ,

$$\mathcal{I}_2 = \sum_{l=0}^{\infty} \frac{\Gamma(l+u, \frac{\lambda}{2})}{2^l \Gamma(l+1) \Gamma(l+u)} \int_0^\infty x^{2l} e^{-\frac{x^2}{2}(1+\frac{2m}{\gamma})} I_1 \left(2m\sqrt{\frac{2}{\gamma}}x \right) dx. \quad (24)$$

Therefore, by substituting [30, eq. (6.643.2)] into (24) and with the aid of [30, eq. (9.220.2)], the following analytic expression for $\overline{P}_{d\kappa-\mu Ext.}$ is deduced,

$$\overline{P}_{d\kappa-\mu Ext.} = \sum_{l=0}^{\infty} \frac{4m^2 \Gamma(l+u, \frac{\lambda}{2}) {}_1F_1 \left(l+1; 2; \frac{4m^2}{\gamma+2m} \right)}{e^{2m} \Gamma(l+u) \left(1 + \frac{2m}{\gamma} \right)^l (2m + \gamma)}. \quad (25)$$

Importantly, the above series can be equivalently expressed in closed-form as follows,

$$\overline{P}_{d\kappa-\mu Ext.} = \frac{4m^2 e^{-2m}}{\gamma + 2m} \left\{ F_A \left(1; 1; 2, 1; \frac{1}{1 + \frac{2m}{\gamma}}, \frac{4m^2}{\gamma + 2m} \right) - \frac{\lambda^u}{u! 2^u} H_A \left(1, u; 1, 2, u, u+1; \frac{\lambda}{2 + \frac{4m}{\gamma}}, -\frac{\lambda}{2}, \frac{4m^2}{\gamma + 2m} \right) \right\} \quad (26)$$

the derivation of (26) is given in APPENDIX B.

C. Square-Law Selection (SLS)

As in the case of (SLS) diversity in $\kappa-\mu$ fading, the average probability for $\kappa-\mu$ Extreme fading is obtained by averaging $P_{d,SLS}$ in [10, eq. (15)] over L independent $\kappa-\mu$ Extreme branches. To this effect, by substituting (22) in (16) and utilizing (24), it follows that Based on this and with the aid of (25), one obtains the following closed-form expression,

$$\begin{aligned}
\overline{P}_{d_{\kappa-\mu Ext.}}^{SLS} &= 1 - \prod_{i=1}^L \{1 - \overline{P}_{d_{\kappa-\mu Ext.}}(\gamma_i)\} \\
&= 1 - \prod_{i=1}^L \left\{ 1 - \frac{4m^2 e^{-2m}}{\overline{\gamma}_i + 2m} \left[F_A \left(1; 1; 2, 1; \frac{1}{1 + \frac{2m}{\overline{\gamma}_i}}, \frac{4m^2}{\overline{\gamma}_i + 2m} \right) \right. \right. \\
&\quad \left. \left. - \frac{\lambda^u}{u! 2^u} H_A \left(1, u; 1, 2, u, u + 1; \frac{\lambda}{2 + \frac{4m}{\overline{\gamma}_i}}, -\frac{\lambda}{2}, \frac{4m^2}{\overline{\gamma}_i + 2m} \right) \right] \right\}. \tag{27}
\end{aligned}$$

D. Collaborative Detection

It is recalled that when the energy detection is performed by n collaborating users, the corresponding average probability of detection is given by $Q_d = 1 - (1 - P_d)^n$. Therefore, for the case of n users collaborating over $\kappa-\mu$ *Extreme* fading, the following relationship is deduced,

$$\begin{aligned}
\overline{Q}_{d_{\kappa-\mu Ext.}} &= 1 - \left[1 - \frac{4m^2 e^{-2m}}{\overline{\gamma} + 2m} \left\{ F_A \left(1; 1; 2, 1; \frac{1}{1 + \frac{2m}{\overline{\gamma}}}, \frac{4m^2}{\overline{\gamma} + 2m} \right) \right. \right. \\
&\quad \left. \left. - \frac{\lambda^u}{u! 2^u} H_A \left(1, u; 1, 2, u, u + 1; \frac{\lambda}{2 + \frac{4m}{\overline{\gamma}}}, -\frac{\lambda}{2}, \frac{4m^2}{\overline{\gamma} + 2m} \right) \right\} \right]^n. \tag{28}
\end{aligned}$$

E. Asymptotic Analysis for small SNR values

One of the major issues in spectrum sensing techniques for cognitive radio is the detection of unknown signals in the low SNR regime. This task is often problematic since for $\text{SNR} \ll 0$ (linear scale) the detector can not typically distinguish the energy of the signal from the energy of the noise unless the number of samples asymptotically scales as $1/\text{SNR}^2$, [38]. Furthermore, the detection becomes significantly harder below -20dB, [39]. In the next Section, it is shown that the $\kappa-\mu$ *Extreme* model characterizes acceptably the extreme fading conditions experienced by the detector even at the low SNR regime.

Therefore, it is considered essential to derive asymptotic expressions for $\overline{\gamma} \ll 0$. To this end, for $\overline{\gamma} \leq -10\text{dB}$ i.e $\overline{\gamma} \leq 0.1$ and given that typically $m \geq 0.5$, it immediately follows that $\overline{\gamma} + 2m \approx 2m$ as well as $1 + 2m/\overline{\gamma} \approx 2m/\overline{\gamma}$ and $2 + 4m/\overline{\gamma} \approx 4m/\overline{\gamma}$. Hence, by substituting

these tight approximations into (25) and (26) and after some basic algebraic manipulations one obtains²,

$$\begin{aligned} \lim_{\bar{\gamma} \rightarrow 0} \overline{P}_{d\kappa-\mu Ext.} &= \sum_{l=0}^{\infty} \frac{\bar{\gamma}^l \Gamma(l + u, \frac{\lambda}{2}) {}_1F_1(l + 1; 2; 2m)}{e^{2m} \Gamma(l + u) 2^{l-1} m^{l-1}} \\ &= \frac{2m}{e^{2m}} \left[F_A \left(1; 1; 2, 1; \frac{\bar{\gamma}}{2m}; 2m \right) - \frac{\lambda^u}{u! 2^u} H_A \left(1, u; 1, 2, u, u + 1; \frac{\lambda \bar{\gamma}}{4m}, -\frac{\lambda}{2}, 2m \right) \right]. \end{aligned} \quad (29)$$

With the aid of the above expression and by recalling that $\overline{P}_d^{SLS} = 1 - \prod_{i=1}^L [1 - \overline{P}_d(\gamma_i)]$ and $Q_d = 1 - (1 - P_d)^n$, asymptotic expressions for small SNR values can be straightforwardly deduced for the case of SLS diversity and collaborative spectrum sensing, namely,

$$\begin{aligned} \lim_{\bar{\gamma} \rightarrow 0} \overline{P}_{d\kappa-\mu Ext.}^{SLS} &= 1 - \prod_{i=1}^L \left\{ 1 - \frac{2m}{e^{2m}} \left[F_A \left(1; 1; 2, 1; \frac{\bar{\gamma}_i}{2m}, 2m \right) \right. \right. \\ &\quad \left. \left. - \frac{\lambda^u}{u! 2^u} H_A \left(1, u; 1, 2, u, u + 1; \frac{\lambda \bar{\gamma}_i}{4m}, -\frac{\lambda}{2}, 2m \right) \right] \right\}. \end{aligned} \quad (30)$$

and

$$\begin{aligned} \lim_{\bar{\gamma} \rightarrow 0} \overline{Q}_{d\kappa-\mu Ext.} &= 1 - \left[1 - \frac{2m}{e^{2m}} \left\{ F_A \left(1; 1; 2, 1; \frac{\bar{\gamma}_i}{2m}, 2m \right) \right. \right. \\ &\quad \left. \left. - \frac{\lambda^u}{u! 2^u} H_A \left(1, u; 1, 2, u, u + 1; \frac{\lambda \bar{\gamma}_i}{4m}, -\frac{\lambda}{2}, 2m \right) \right\} \right]^n. \end{aligned} \quad (31)$$

respectively.

V. RESULTS AND DISCUSSIONS

This section is devoted to the description of the behaviour of an energy detection in $\kappa-\mu$ and $\kappa-\mu$ *Extreme* fading channels. Its performance is quantified for different scenarios of interest through both \overline{P}_d versus $\bar{\gamma}$ curves and complementary receiver operating characteristics (ROC) curves (P_m versus P_f).

Fig. 1 demonstrates \overline{P}_d vs $\bar{\gamma}$ curves for $\kappa-\mu$ fading for different κ and μ values with $P_f = 0.1$ and $u = 2$. One can observe that the energy detector performs better as κ and μ increase due

²The value of $\bar{\gamma}$ is in linear scale when dB is not indicated.

to the higher dominance of the LOS component and the advantage of the multipath effect, respectively. For example, for the case of $\bar{\gamma} = 15 \text{ dB}$ and $\kappa = 1.0$ (fixed), the \bar{P}_d for $\mu = 0.7$ is about 10% higher than for $\mu = 0.5$. In the same context, when $\mu = 0.7$ (fixed), the \bar{P}_d for $\kappa = 3.0$ is 9% higher than for the case of $\kappa = 1.0$.

As the value of $\bar{\gamma}$ decreases to negative values, the effect of varying κ and μ is shown to reduce. This can be also observed in Fig. 2 which illustrates complementary ROC curves for the case of a five branch SLS diversity assuming $u = 2$, $\mu = 0.5$ and $\kappa = 1.0$ and average SNR for each branch set to $\bar{\gamma}_1 = 0 \text{ dB}$, $\bar{\gamma}_2 = 1 \text{ dB}$, $\bar{\gamma}_3 = 2 \text{ dB}$, $\bar{\gamma}_4 = 3 \text{ dB}$ and $\bar{\gamma}_5 = 4 \text{ dB}$. Clearly, the effect of each fading scenario on \bar{P}_m is greater as $\bar{\gamma}$ increases while the performance of the detector is highly depended on the number of branches. For example, the value of P_m for $L = 1$ and $P_f = 0.15$ (fixed), is about 80% larger compared to the case of $L = 5$.

Fig. 3 illustrates the complementary ROC for energy detection with up to eight collaborating users. The fading scenarios considered are the same as in the previous case while the average SNR is set to $\bar{\gamma} = 3 \text{ dB}$. As expected, the performance of the energy detector improves as the number of users increase.

Regarding the effect of $\kappa-\mu$ *Extreme* fading conditions, Fig. 4 illustrates the behaviour of the energy detector with respect to the SNR. Evidently, the performance of the detector is highly dependant upon the severity of fading and improves substantially as m increases. Indicatively, by increasing the fading severity from $m = 0.7$ to $m = 0.5$ for $\bar{\gamma} = 10 \text{ dB}$ and $P_f = 0.1$, renders a 16% performance reduction.

Fig. 5 demonstrates the significant performance improvement when the SLS diversity scheme is employed. Evidently, for $P_f = 0.2$, the value of \bar{P}_m , over the single branch operation, reduces by about 30% and 58% for $L = 2$ and $L = 3$, respectively, for both $m = 0.6$ and $m = 1.8$.

In the case of collaborating spectrum sensing with up to four users for $u = 2$, $\bar{\gamma} = 3 \text{ dB}$, the value of \bar{Q}_m reduces as the number of users increases for any value of m . For example, Fig. 6 illustrates that for a single user detection for $P_f = 0.2$ and $m = 0.6$, the value of \bar{P}_m is 67% higher compare to the case that $n = 4$.

It is also important to note that the $\kappa-\mu$ *Extreme* fading model can provide adequate characterization of the fading effect in the low SNR regime. It is recalled that energy detection in $\bar{\gamma} = 20 \text{ dB}$ is a challenging task since the detector can not distinguish unknown signals with low power from noise power. Fig. 7, depicts the behaviour of the energy detector in $\kappa-\mu$ *Extreme*

fading conditions with respect to the fading severity and SLS diversity. It is clearly seen that the value of P_m decreases substantially as the number of diversity branches increases. For example, for $P_f = 0.3$, $u = 2$, $\bar{\gamma} = 20dB$ and $L = 6$, it is seen that $0.18 \leq P_m \leq 0.28$ for $0.5 \leq m \leq 1$ and $P_m < 0.17$ for $m > 1$. For larger numbers of branches ($L > 6$), the value of P_m continues to reduce but at a much smaller rate and thus a small benefit will be gained at the expense of significantly higher complexity.

Finally, the dramatic effect of the different fading conditions modelled by the $\kappa-\mu$ and $\kappa-\mu$ *Extreme* distributions is also demonstrated through comparisons with results from existing works. For example, for $\bar{\gamma} = 10dB$ and $u = 2$, $P_f = 0.1$ in Fig. 1, one obtains $\bar{P}_d = 0.77$ for Rayleigh fading in [10], $\bar{P}_d = 0.95$ for light fading (yellow curve) and $\bar{P}_d = 0.68$ for severe fading conditions (blue curve). Similarly, for $\bar{\gamma} = 5dB$ and $u = 2$, $P_f = 0.1$ in Fig. 4, one obtains $\bar{P}_d = 0.51$ for Rayleigh fading and $\bar{P}_d = 0.59$ for $m = 0.5$ (yellow curve) and $\bar{P}_d = 0.4$ for $m = 3.0$ (blue curve). It is also evident that the results lie within a significantly wider range in comparison with Nakagami- m fading as results in [17] since the value of \bar{P}_d is smaller even for larger values of u and $\bar{\gamma}$. However, apart from the differences on the behaviour of \bar{P}_d over different fading conditions, there are also differences in the algebraic representation between the proposed and recently reported results. Specifically, the works in [17]–[19], [22] represent the average probability of detection in a semi-analytic form due to the presence n^{th} derivative term. This renders the derived expressions in the present work more straightforward to use as well as less computationally laborious and exhaustive.

VI. CONCLUSION

This work analyzed of the performance of energy detection in $\kappa-\mu$ and $\kappa-\mu$ *Extreme* fading channels. Novel analytic expressions were derived for the average probability of detection for both cases. The overall performance of the detector is largely affected by the value of the corresponding fading parameters since it is very sensitive even at small variations particularly as the average SNR increases. It was also shown that a significant performance improvement is achieved in both severe and moderate fading conditions as the number of diversity branches or number of users increases. Furthermore, it is shown that the $\kappa-\mu$ *Extreme* fading model provides adequate fading characterization of the fading effect in the low SNR regime and thus improves the performance of the energy detector. As a result, the offered results are useful in quantifying

the effect of fading in energy detection spectrum sensing which will lead in improved and/or more energy efficient cognitive radio-based communication systems.

APPENDIX A

DERIVATION OF EQUATION (15)

According to [30, eq. (8.354.2)], the upper incomplete gamma function can be expressed as $\Gamma(a, x) \triangleq \Gamma(a) - \sum_{n=0}^{\infty} \frac{(-1)^n x^{a+n}}{n!(a+n)}$. By also recalling that $\Gamma(a+1) = a!$ and ${}_1F_1(a; b; x) \triangleq \sum_{n=0}^{\infty} \frac{(a)_n x^n}{(b)_n n!}$ and performing the necessary change of variables, equation (15) can be re-written as follows:

$$\begin{aligned} \overline{P}_{d\kappa-\mu} &= \underbrace{\sum_{l=0}^{\infty} \sum_{j=0}^{\infty} \frac{\mu^\mu (1+\kappa)^\mu \bar{\gamma}^l \Gamma(\mu+l+j) \kappa^j (1+\kappa)^j \mu^{2j} e^{-\mu\kappa}}{l! \Gamma(\mu+l) (\bar{\gamma} + \mu + \kappa \mu)^{\mu+l} j! (\bar{\gamma} + \mu(1+\kappa))^j}}_{\mathcal{I}_3} \\ &\quad - \underbrace{\sum_{l=0}^{\infty} \sum_{i=0}^{\infty} \sum_{j=0}^{\infty} \frac{(-1)^i \mu^{\mu+2j} (1+\kappa)^{\mu+j} \Gamma(\mu+l+j) \lambda^{l+i+u} \bar{\gamma} \kappa^j e^{-\mu\kappa}}{l! j! i! \Gamma(l+u) 2^{l+i+u} \Gamma(\mu+j) (l+i+u) (\bar{\gamma} + \mu + \kappa \mu)^{\mu+l+j}}}_{\mathcal{I}_4} \end{aligned} \quad (A.1)$$

By recalling that the Pochhammer symbol is defined as $(a)_n \triangleq \Gamma(a+n)/\Gamma(a)$, the Gamma functions in \mathcal{I}_3 and \mathcal{I}_4 can be expressed as $\Gamma(\mu+l+j) = (\mu)_{l+j} \Gamma(\mu)$, $\Gamma(\mu+l) = (\mu)_l \Gamma(\mu)$, $\Gamma(l+u) = (u)_l \Gamma(u)$ and $\Gamma(\mu+j) = (\mu)_j \Gamma(\mu)$. Furthermore, the $(l+i+u)$ term in \mathcal{I}_4 can be equivalently expressed as,

$$l+i+u = \frac{(l+i+u)!}{(l+i+u-1)!} = \frac{\Gamma(l+i+u+1)}{\Gamma(l+i+u)} \quad (A.2)$$

By expressing each Gamma function in terms of the Pochhammer symbol it follows that,

$$l+i+u = \frac{(u+1)_{l+i} \Gamma(u+1)}{(u)_{l+i} \Gamma(u)} = \frac{(u+1)_{l+i} (u)_1}{(u)_{l+i}} \quad (A.3)$$

By substituting accordingly in \mathcal{I}_3 and \mathcal{I}_4 and carrying our some long but basic algebraic manipulations, one obtains,

$$\overline{P}_{d\kappa-\mu} = \frac{\mu^\mu (1+\kappa)^\mu e^{-\mu\kappa}}{(\bar{\gamma} + \mu + \kappa \mu)^\mu} \underbrace{\sum_{l=0}^{\infty} \sum_{j=0}^{\infty} \frac{(\mu)_{l+j}}{(\mu)_j} \frac{\left(\frac{\bar{\gamma}}{\bar{\gamma} + \mu + \kappa \mu}\right)^l}{l!} \frac{\left(\frac{\kappa(1+\kappa)\mu^2}{\bar{\gamma} + \mu + \kappa \mu}\right)^j}{j!}}_{\mathcal{I}_5} \quad (A.4)$$

$$\frac{\mu^\mu (1 + \kappa)^\mu \lambda^u e^{-\mu\kappa}}{2^u u! (\bar{\gamma} + \mu + \kappa \mu)^\mu} \underbrace{\sum_{l=0}^{\infty} \sum_{i=0}^{\infty} \sum_{j=0}^{\infty} \frac{(\mu)_{l+j} (u)_{l+i}}{(u)_l (u+1)_{l+i} (\mu)_j} \frac{\left(\frac{\lambda \bar{\gamma}}{2(\bar{\gamma} + \mu + \kappa \mu)}\right)^l}{l!} \frac{\left(-\frac{\lambda}{2}\right)^i}{i!} \frac{\left(\frac{\kappa(1+\kappa)\mu^2}{\bar{\gamma} + \mu(1+\kappa)}\right)^j}{j!}}_{\mathcal{I}_6}$$

Importantly, the algebraic form of \mathcal{I}_5 is the same as the representation of the Lauricella hypergeometric function in [30, eq. (9.19)], [36, eq. (1)]. Similarly \mathcal{I}_6 can be expressed in terms of the complete triple hypergeometric function of the first kind in [35, eq. (1.1)]. To this effect, by performing the necessary variable transformation, equation (15) is deduced.

APPENDIX B

DERIVATION OF EQUATION (26)

The proof follows immediately from APPENDIX A.

REFERENCES

- [1] S. Haykin, "Cognitive radio: Brain-empowered wireless communications", in *IEEE J. Select. Areas Commun.* vol. 23, no. 2, pp. 201-220, Feb. 2005.
- [2] S. Haykin, M. Moher, "Modern Wireless Communications", *Prentice-Hall*, Inc. Upper Saddle River, NJ, USA, 2004.
- [3] V. K. Bargava, E. Hossain, "Cognitive Wireless Communication Networks", *Springer-Verlag*, Berlin, Heidelberg 2009.
- [4] H. Urkowitz, "Energy detection of unknown deterministic signals", *Proceedings of the IEEE*, vol. 55, no. 4, pp. 523-531, 1967.
- [5] V. I. Kostylev, "Energy detection of signal with random amplitude", in *Proc. IEEE Int. Conf. on Communications (ICC)*, vol. 3, pp. 1606-1610, May 2002.
- [6] S. Atapattu, C. Tellambura and hai Jiang, "Performance of energy detection: A complementary AUC approach", in *Proc. IEEE Globecom '10*, pp. 1-5, Dec. 2010.
- [7] A. Rabbachin, T. Q. S. Quek, P. C. Pinto, I. Oppermann, M. Z. Win, "UWB energy detection in the presence of multiple narrowband interferers", in *Proc. IEEE Int. Conf. Ultra Wideband, (ICUWB '07)*, pp. 857-862, Sep. 2007.
- [8] S. P. Herath, N. Rajatheva, C. Tellambura, "On the energy detection of unknown deterministic signal over Nakagami channels with selection combining", in *Proc. IEEE CCECE '09*, pp. 745-749, May 2009.
- [9] A. Ghasemi, E. S. Sousa, "Spectrum sensing in cognitive radio networks: Requirements, challenges and design trade-offs", in *IEEE Comm. Magazine*, pp. 32-39, Apr. 2008.
- [10] F. F. Digham, M. S. Alouini, M. K. Simon, "On the energy detection of unknown signals over fading channels", in *IEEE Trans. Commun.* vol. 55, no. 1, pp. 21-24, Jan. 2007.
- [11] S. P. Herath, N. Rajatheva, "Analysis of equal gain combining in energy detection for cognitive radio over Nakagami channels", in *Proc. IEEE Globecom '08*, pp. 2972-2976, Dec. 2008.
- [12] A. Ghasemi, E.S. Sousa, "Collaborative spectrum sensing for opportunistic access in fading environments", in *Proc. DySpan '05*, pp. 131-136, Nov. 2005.

- [13] A. Ghasemi, E.S. Sousa, "Impact of User Collaboration on the Performance of Sensing-Based Opportunistic Spectrum Access", in *Proc. IEEE VTC-fall '06*, pp. 1-6, Sep. 2006.
- [14] A. Ghasemi, E.S. Sousa, "Asymptotic Performance of collaborative spectrum sensing under correlated Log-normal shadowing", in *IEEE Comm. Letters*, vol. 11, no. 1, pp. 34-36, Jan. 2007.
- [15] S. Atapattu, C. Tellambura, H. Jiang, "Relay based cooperative spectrum sensing in cognitive radio networks", in *Proc. IEEE Globecom '09*, pp. 4310-4314, Nov.-Dec. 2009.
- [16] S. Atapattu, C. Tellambura, H. Jiang, "Energy detection based cooperative spectrum sensing in cognitive radio networks", in *IEEE Trans. on Wirel. Commun.*, vol. 10, no. 4, pp. 1232-1241, Apr. 2011.
- [17] S. P. Herath, N. Rajatheva, C. Tellambura, "Energy detection of unknown signals in fading and diversity reception", in *IEEE Trans. Commun.*, vol. 59, no. 9, pp. 2443-2453, Sep. 2011.
- [18] K. T. Hemachandra, N. C. Beaulieu, "Novel analysis for performance evaluation of energy detection of unknown deterministic signals using dual diversity", in *Proc. IEEE VTC-Fall '11*, pp. 1-5, Sep. 2011.
- [19] S. Atapattu, C. Tellambura, H. Jiang, "Spectrum Sensing via Energy Detector in Low SNR", *Proc. IEEE ICC '11*, pp. 1-5, June 2011.
- [20] K. Ruttik, K. Koufos and R. Jantti, "Detection of unknown signals in a fading environment", in *IEEE Comm. Letters*, vol. 13, no. 7, pp. 498-500, July 2009.
- [21] S. Atapattu, C. Tellambura, H. Jiang, "Performance of an energy detector over channels with both multipath fading and shadowing", in *IEEE Trans. on Wirel. Commun.* vol. 9, no. 12, pp. 3662-3670, Dec. 2010.
- [22] S. Atapattu, C. Tellambura, H. Jiang, "Energy Detection of Primary signals over $\eta-\mu$ fading channels", in *Proc. 4th ICIS '09*, pp. 1-5, Dec. 2009.
- [23] M. D. Yacoub, "The $\kappa-\mu$ distribution and the $\eta-\mu$ distribution", in *IEEE Antennas and Propagation Magazine*, vol. 49, no. 1, pp. 68-81, Feb. 2007.
- [24] G. S. Rabelo, U. S. Dias, M. D. Yacoub, "The $\kappa-\mu$ Extreme distribution: Characterizing severe fading conditions", in *Proc. SBMO/IEEE MTT-S IMOC*, pp. 244-248, Nov. 2009.
- [25] G. S. Rabelo, U. S. Dias, M. D. Yacoub, "The $\kappa-\mu$ Extreme distribution", in *IEEE Transactions on Communications*, vol. 59, no. 10, pp. 2776-2785, Oct. 2011.
- [26] M. Abramowitz and I. A. Stegun, "Handbook of Mathematical Functions With Formulas, Graphs, and Mathematical Tables.", *New York: Dover*, 1974.
- [27] J. I. Marcum, "A statistical theory of target detection by pulsed radar: Mathematical appendix", *RAND Corp., Santa Monica, Research memorandum*, CA, 1948.
- [28] V. M. Kapinas, S. K. Mihos, and G. K. Karagiannidis, "On the monotonicity of the generalized Marcum and Nuttall Q-functions", in *IEEE Trans. Inf. Theory*, vol. 55, no. 8, pp. 3701-3710, Aug. 2009.
- [29] P. C. Sofotasios, S. Freear, "Novel expressions for the Marcum and one Dimensional Q-Functions", in *Proc. of the 7th ISWCS '10*, pp. 736-740, Sep. 2010.
- [30] I. S. Gradshteyn and I. M. Ryzhik, "Table of Integrals, Series, and Products", 7th ed. *New York: Academic*, 2007.
- [31] E. A. Neasmith and N. C. Beaulieu, "New results on selection diversity", in *IEEE Trans. Commun.* vol. 46, no. 5, pp. 695-704, May 1998.
- [32] M. D. Yacoub, D. B. da Costa, U. S. Dias, and G. Fraidenraich, "Joint Statistics for Two Correlated Weibull Variates", in *IEEE Ant. and Wirel. Prop. Letters*, vol. 4, pp. 129-132, 2005.
- [33] H. M. Srivastava, Hypergeometric functions of three variables, in *Ganita*, vol. 5, no. 1, pp. 77-91, 1954.

- [34] S. Saran, Some integrals representing triple hypergeometric functions, in *Rend. Circ. Mat. Palermo*, Ser. 2, vol. 16, pp. 99-115, 1967.
- [35] J. Choi, A. Hasanov, H. M. Srivastava and M. Turaev, Integral representations for Srivastava's triple hypergeometric functions, in *Taiwanese Journal of Mathematics*, vol. 15, no. 6, pp. 2751-2762, Dec. 2011.
- [36] Q. Shi and Y. Karasawa, Some Applications of Lauricella Hypergeometric Function F_A in Performance Analysis of Wireless Communications, in *IEEE Communication Letters*, vol. 16, no. 5, pp. 581-584, May 2012.
- [37] M. K. Simon and M. -S. Alouni, "Digital Communication over Fading Channels", *2nd Edition*, New York: Wiley, 2005.
- [38] R. Tandra, "Fundamental limits on detection in low SNR, *M.S. thesis, Dept. Elect. Eng., Univ. CA, Berkeley*, 2005.
- [39] D. Cabric, "Addressing the Feasibility of Cognitive Radios", in *Signal processing Magazine*, pp. 85-93, Nov. 2008.
- [40] P. Pawelczak, K. Nolan, L. Doyle, S. Oh and D. Cabric, "Cognitive radio: Ten years of experimentation and development", in *IEEE Commun. Magazine*, vol. 49, no. 3, pp. 90-100, Mar. 2011.
- [41] P. C. Sofotasios, "On Special Functions and Composite Statistical Distributions and Their Applications in Digital Communications over Fading Channels", *Ph.D Dissertation*, University of Leeds, UK, 2010.

LIST OF FIGURES

Figure 1: \bar{P}_d vs $\bar{\gamma}$ for i.i.d κ - μ fading with $P_f = 0.1$, $u = 2$ and different values for κ and μ .

Figure 2: Complementary ROC curves for SLS diversity in κ - μ fading for different κ , μ and L branches with $u = 2$, $\bar{\gamma}_1 = 0$ dB, $\bar{\gamma}_2 = 1$ dB, $\bar{\gamma}_3 = 2$ dB, $\bar{\gamma}_4 = 3$ dB and $\bar{\gamma}_5 = 4$ dB.

Figure 3: Complementary ROC curves for κ - μ fading with $u = 2$, $\kappa = 3$, $\mu = 1.8$, $\bar{\gamma} = 3$ dB and n collaborating users.

Figure 4: \bar{P}_d vs $\bar{\gamma}$ for different m values under i.i.d κ - μ Extreme fading with $P_f = 0.1$ and $u = 2$.

Figure 5: Complementary ROC curves for SLS based κ - μ Extreme fading for different m and L branches with $u = 2$, $\bar{\gamma}_1 = -2$ dB, $\bar{\gamma}_2 = 0$ dB and $\bar{\gamma}_3 = 2$ dB.

Figure 6: Complementary ROC curves for κ - μ Extreme fading with different m values, $u = 2$, $\bar{\gamma} = 3$ dB and n collaborating users.

Figure 7: \bar{P}_m vs m for κ - μ Extreme fading with $P_f = 0.3$, $u = 2$ and $\bar{\gamma} = -20$ dB and L diversity branches.

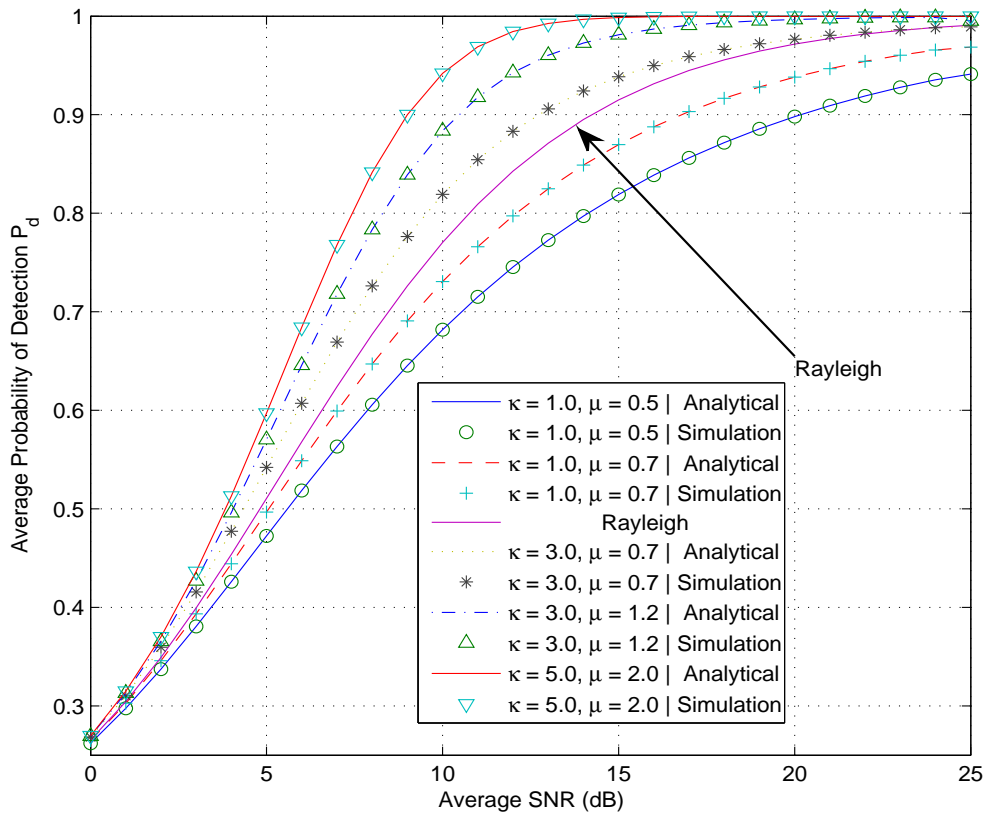


Fig. 1. \bar{P}_d vs $\bar{\gamma}$ for i.i.d κ - μ fading with $P_f = 0.1$, $u = 2$ and different values for κ and μ .

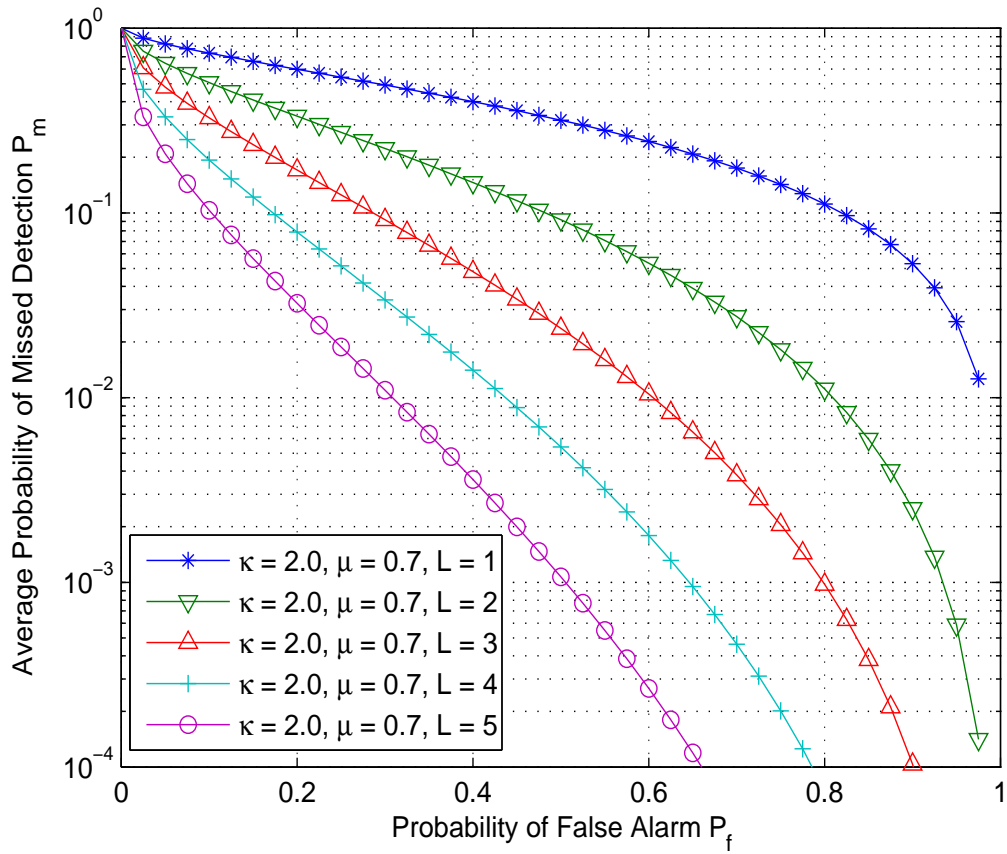


Fig. 2. Complementary ROC curves for SLS diversity in κ - μ fading for different κ , μ and L values with $u = 2$, $\bar{\gamma}_1 = 0$ dB, $\bar{\gamma}_2 = 1$ dB, $\bar{\gamma}_3 = 2$ dB, $\bar{\gamma}_4 = 3$ dB and $\bar{\gamma}_5 = 4$ dB.

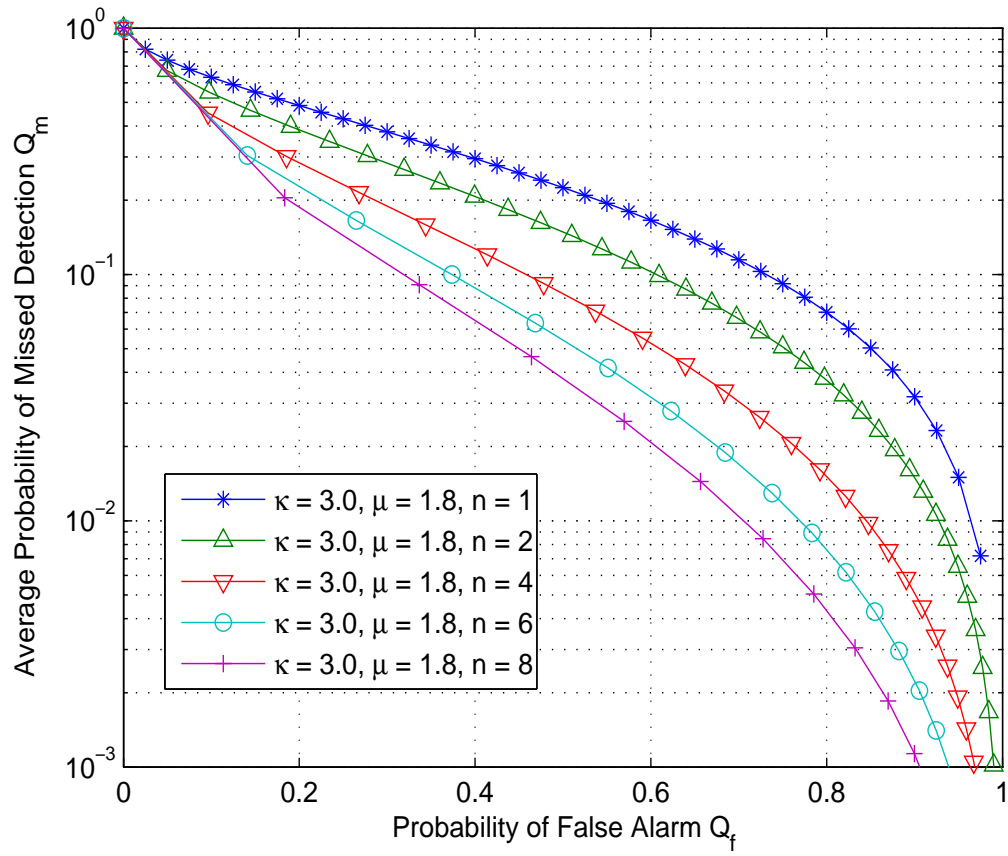


Fig. 3. Complementary ROC curves for κ - μ fading with $u = 2$, $\kappa = 3$, $\mu = 1.8$, $\bar{\gamma} = 3$ dB and n collaborating users.

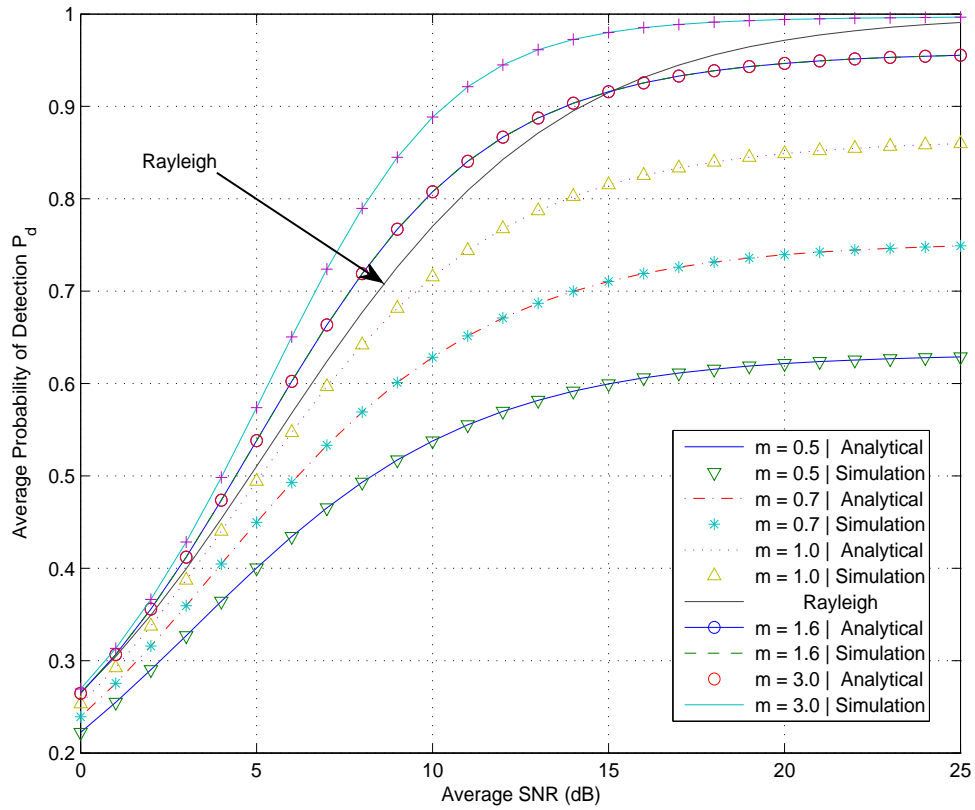


Fig. 4. \bar{P}_d vs $\bar{\gamma}$ for different m values under i.i.d κ - μ Extreme fading with $P_f = 0.1$ and $u = 2$.

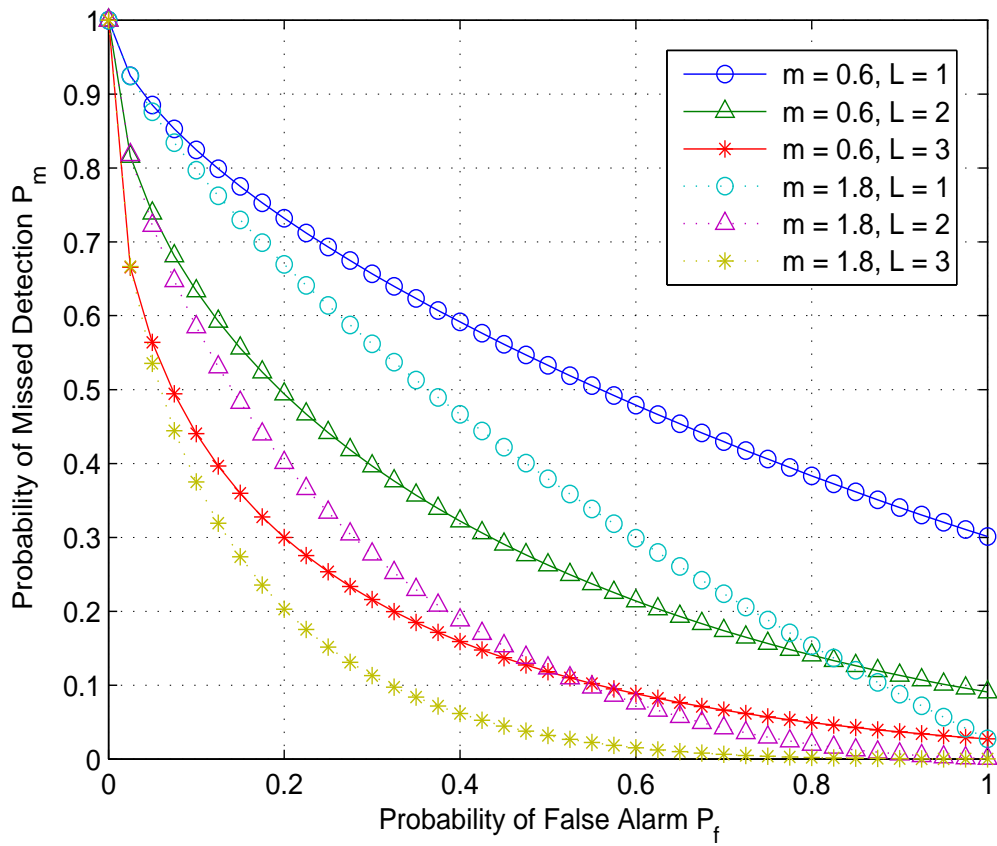


Fig. 5. Complementary ROC curves for SLS based κ - μ Extreme fading for different m and L values with $u = 2$, $\bar{\gamma}_1 = -2$ dB, $\bar{\gamma}_2 = 0$ dB and $\bar{\gamma}_3 = 2$ dB.

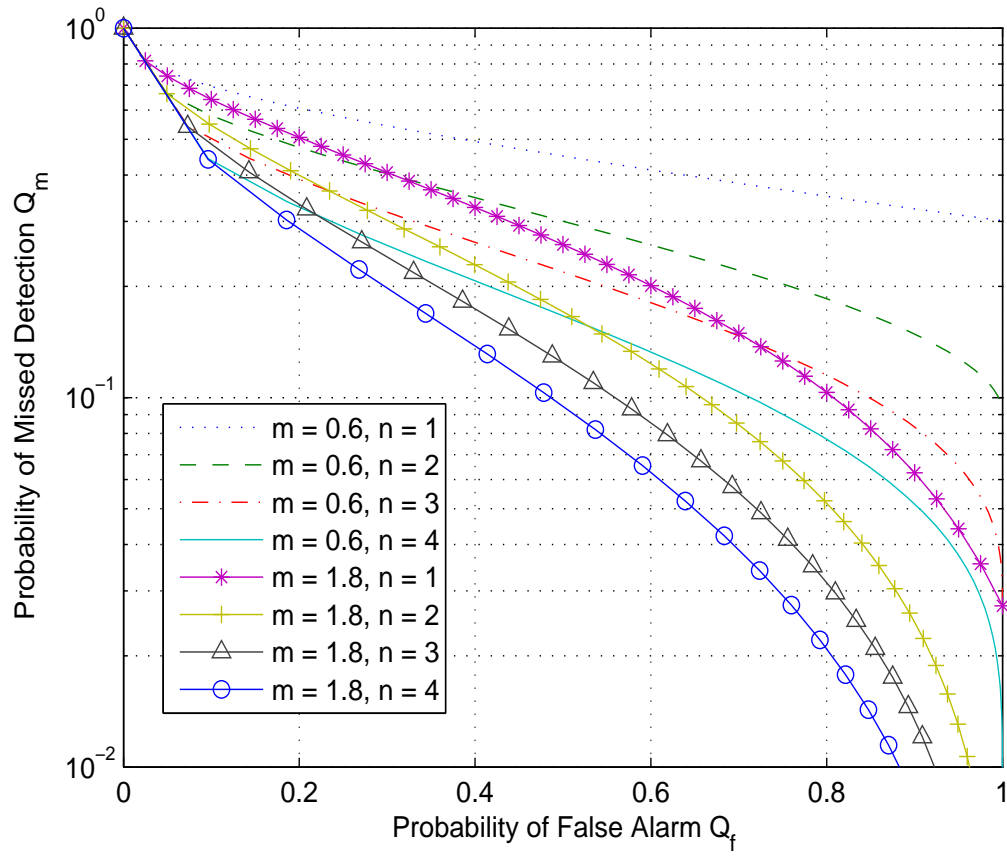


Fig. 6. Complementary ROC curves for κ - μ Extreme fading with different m values, $u = 2$, $\bar{\gamma} = 3$ dB and n collaborating users.

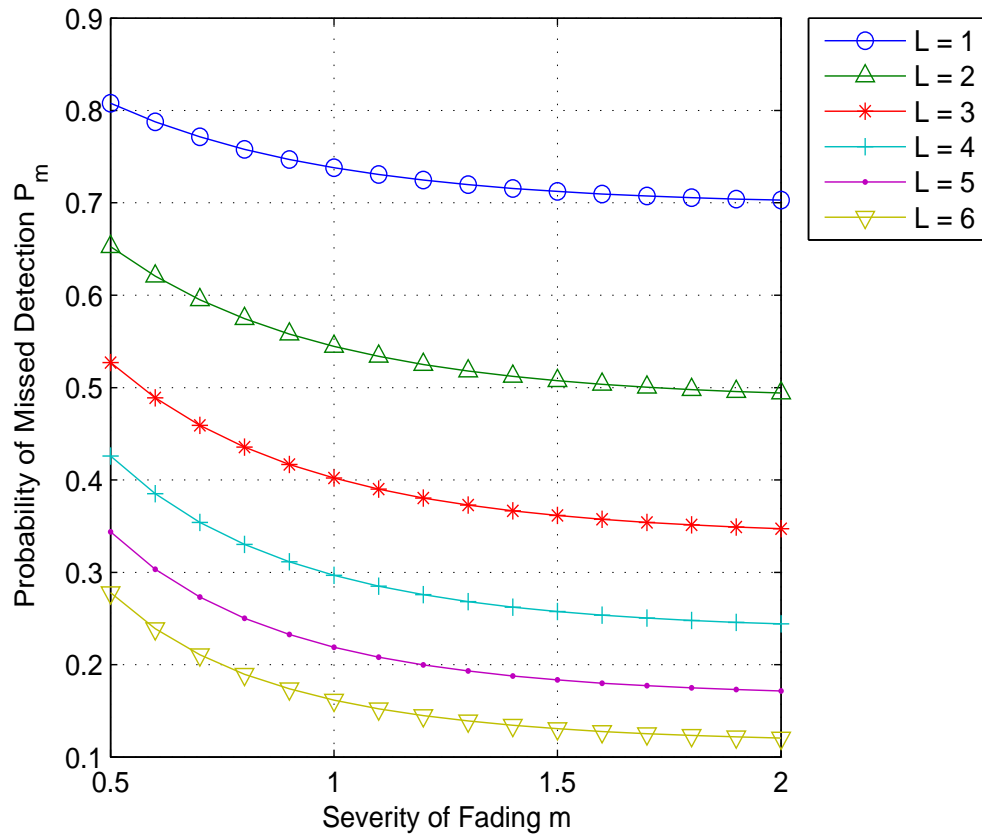


Fig. 7. \bar{P}_m vs m for κ - μ Extreme fading with $P_f = 0.3$, $u = 2$ and $\bar{\gamma} = -20$ dB and L diversity branches.